Struck, M., Jansen, J.D., Fujioka, T., Codilean, A.T., Fink, D., Egholm, D.L., Fülöp, R.-H., Wilcken, K.M., and Kotevski, S., 2017, Soil production and transport on postorogenic desert hillslopes quantified with ^{10}Be and ^{26}Al: GSA Bulletin, https://doi.org/10.1130/B31767.1.

Data Repository

Figure DR1: Sampled bedrock at A) Mt Margaret (NIL-BR1), B) Coongra, and C) Pioneer. Samples at Mt Margaret and Pioneer are amalgamated from 10 and 15 chips, respectively. The Coongra sample was taken from an exfoliated surface.

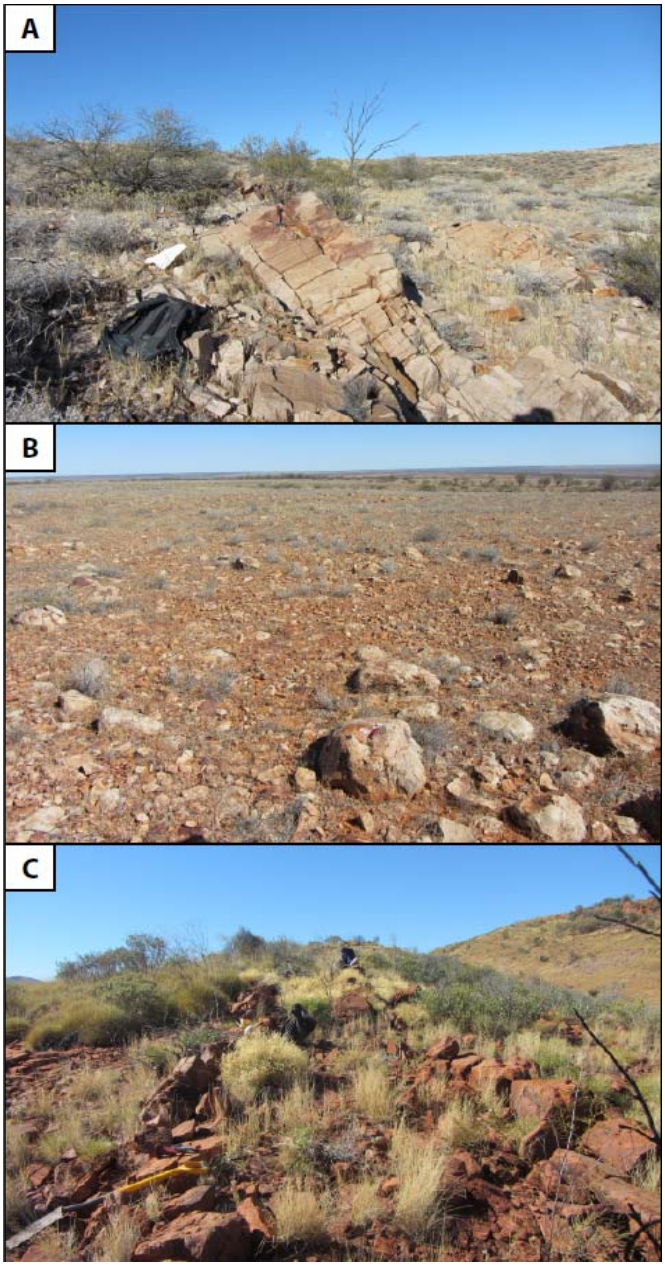

Figure DR2: Exfoliated hilltop bedrock at Coongra and examples for gibber-covered, gently dipping slope in the background.

Figure DR3: Smooth, rounded hills in the Western MacDonnell Ranges. Bedrock slabs are cropping out on the hilltops (arrows). Development of concave slopes and evenly spaced gullies intersecting strongly weathered Cambrian Arumbera sandstone.

Figure DR4: Examples of slope surface images used for digital grain analyses: (A) Mt Margaret, (B) Coongra, (C) Pioneer. Scales used are one staff segment (17.5 cm) and a pen (14.3 cm), respectively. Grain boundaries were mapped where gridlines intersect.

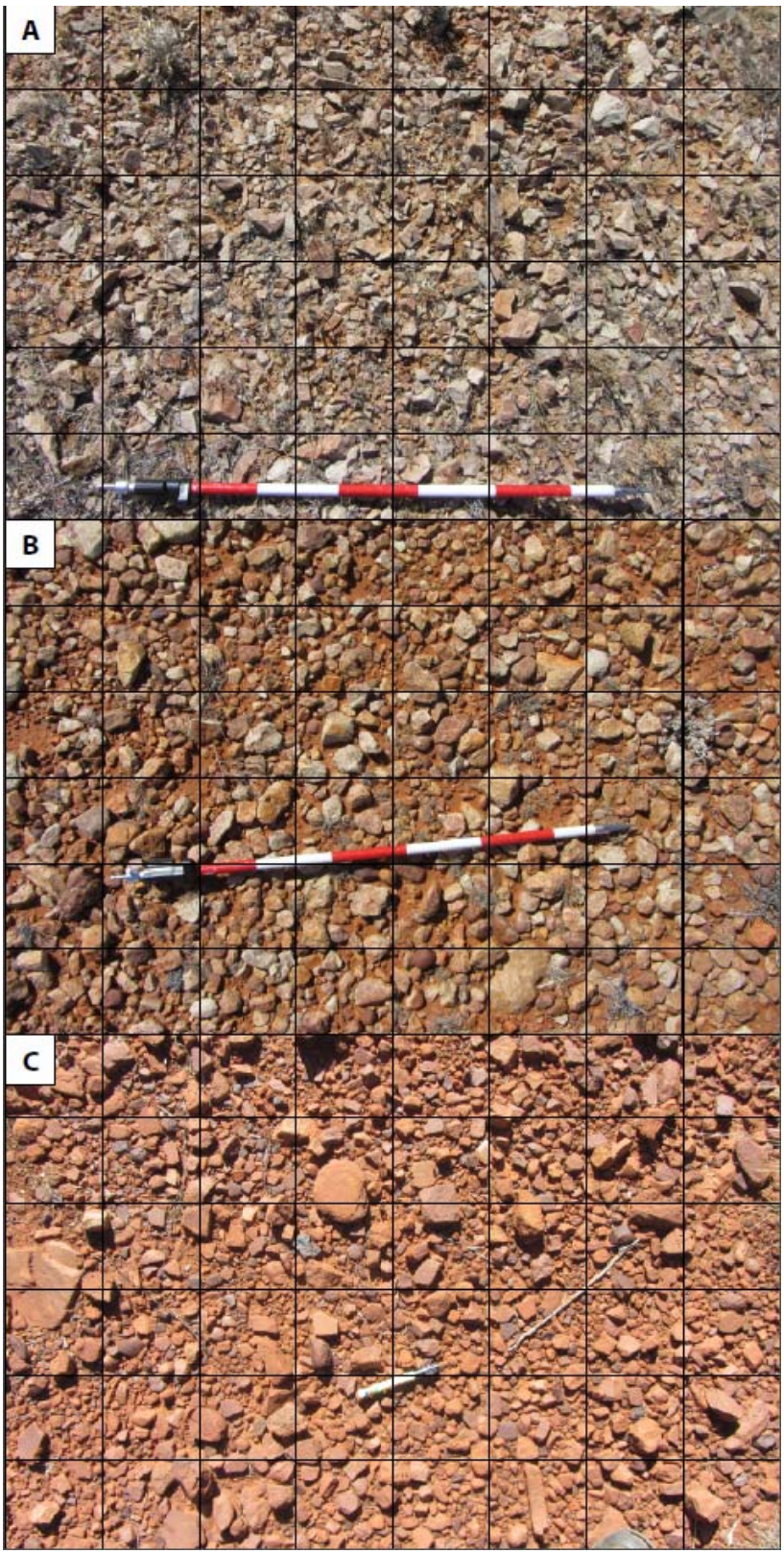

Figure DR5: Illustration of parabolic character of Mt Margaret hillslope by best-fit parabola approximation. Gray diamonds are survey locations. Dashed vertical line and arrow indicate sampled transect section on the right.

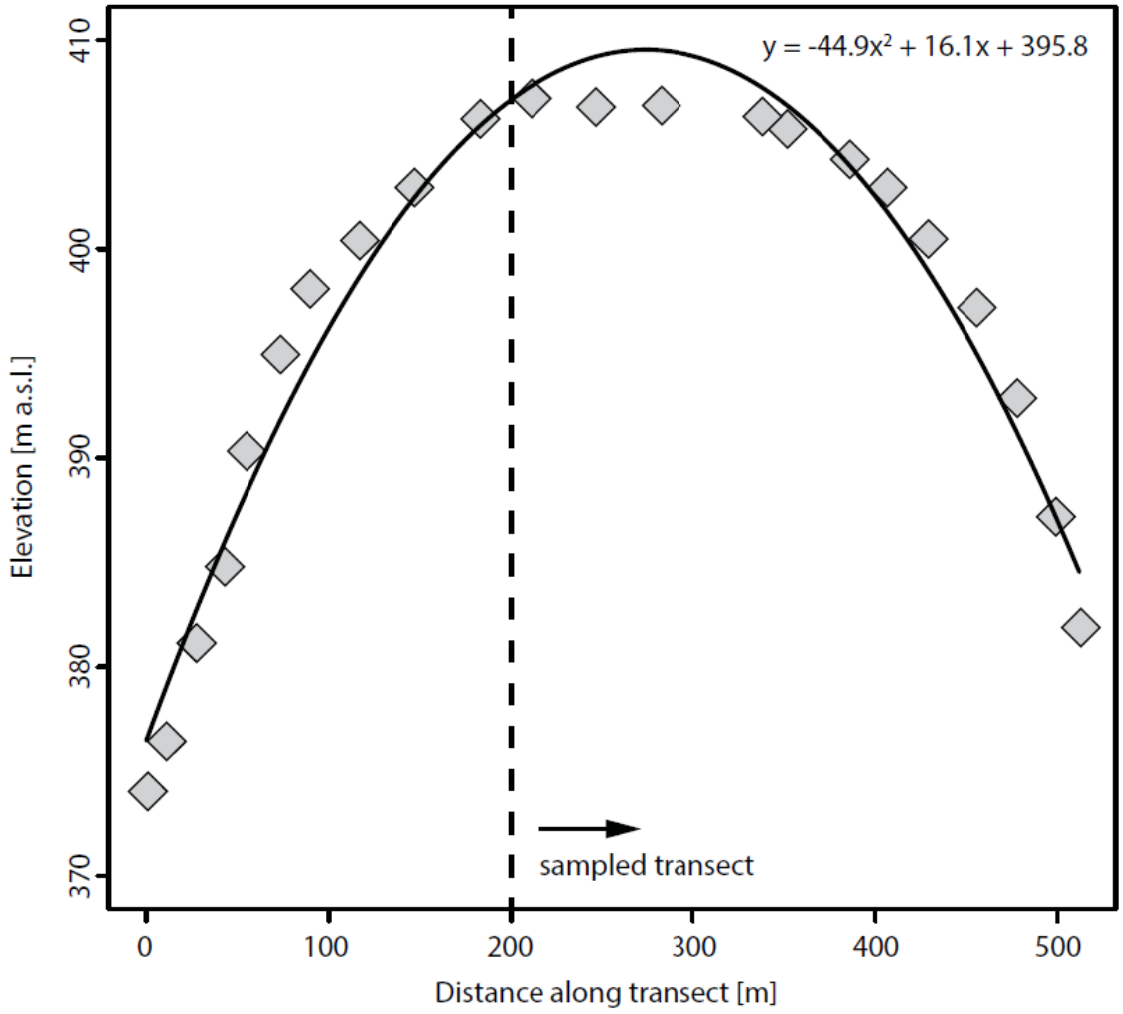

Figure DR6: X-ray diffractogram example of the clay fraction extracted from fine-grained material covering the Mt Margaret plateau pit (here: 50 cm depth). The red curve represents the air-dried sample and the blue curve represents the glycolated sample. Swelling clays are responsible for the shift of peaks towards lower degrees 2-Theta values in the glycolated sample compared to the air-dried sample. The pattern present here indicates illite-smectite mixed-layer swelling clay.

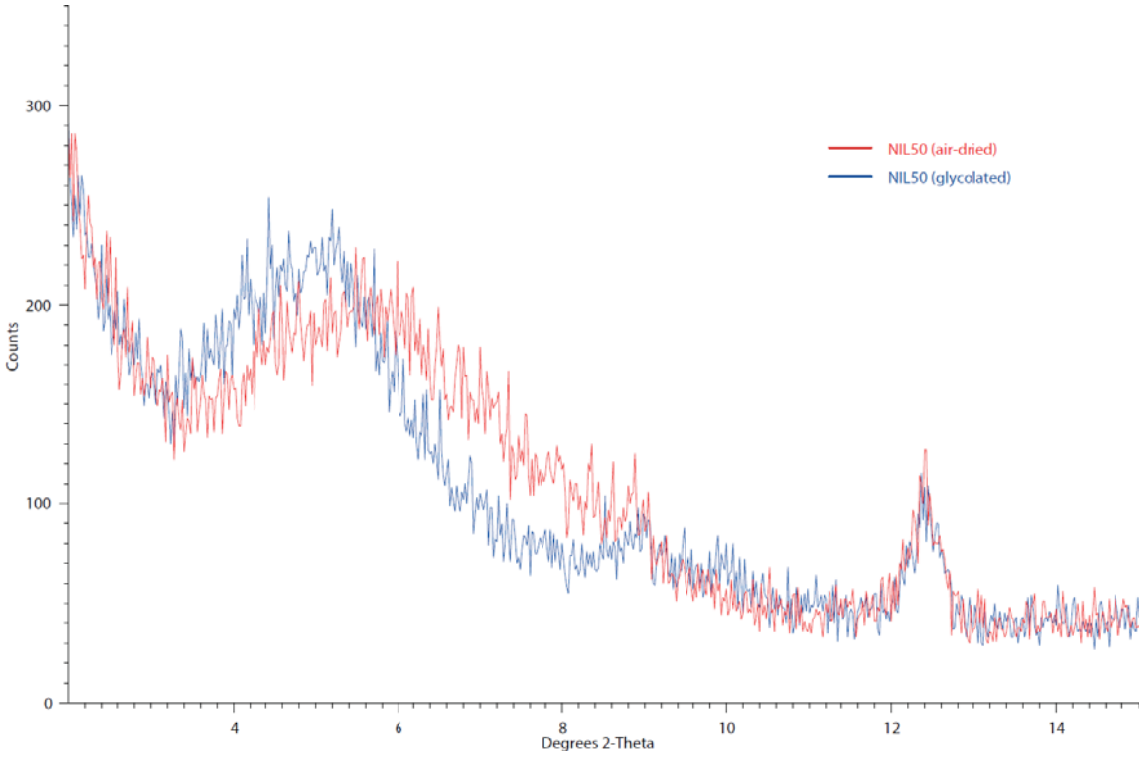

Figures DR7: The MC4 (4-parameter) Monte Carlo-based inversion model outputs (panels I-XI). Colors correspond to models with slow (blue) to fast (red) erosion rates. A) The $^{26}Al/^{10}Be$ (±1σ uncertainty) domain that defines the accepted forward models (except for sample TD-TS1 where ±3σ applies). B) Exhumation paths of accepted models spanning the past 5 m.y. Note the rapid acceleration that occurs when particles detach from bedrock and migrate upwards to the soil surface (i.e. two-speed exhumation). Frequency distributions of accepted models are shown for the four free-parameters: C) Gibber upward-migration time from base of soil to surface; D) Gibber arrival time at soil surface; E) Bedrock erosion rate at the base of the soil, and F) Soil thickness.

I

NIL-TS0

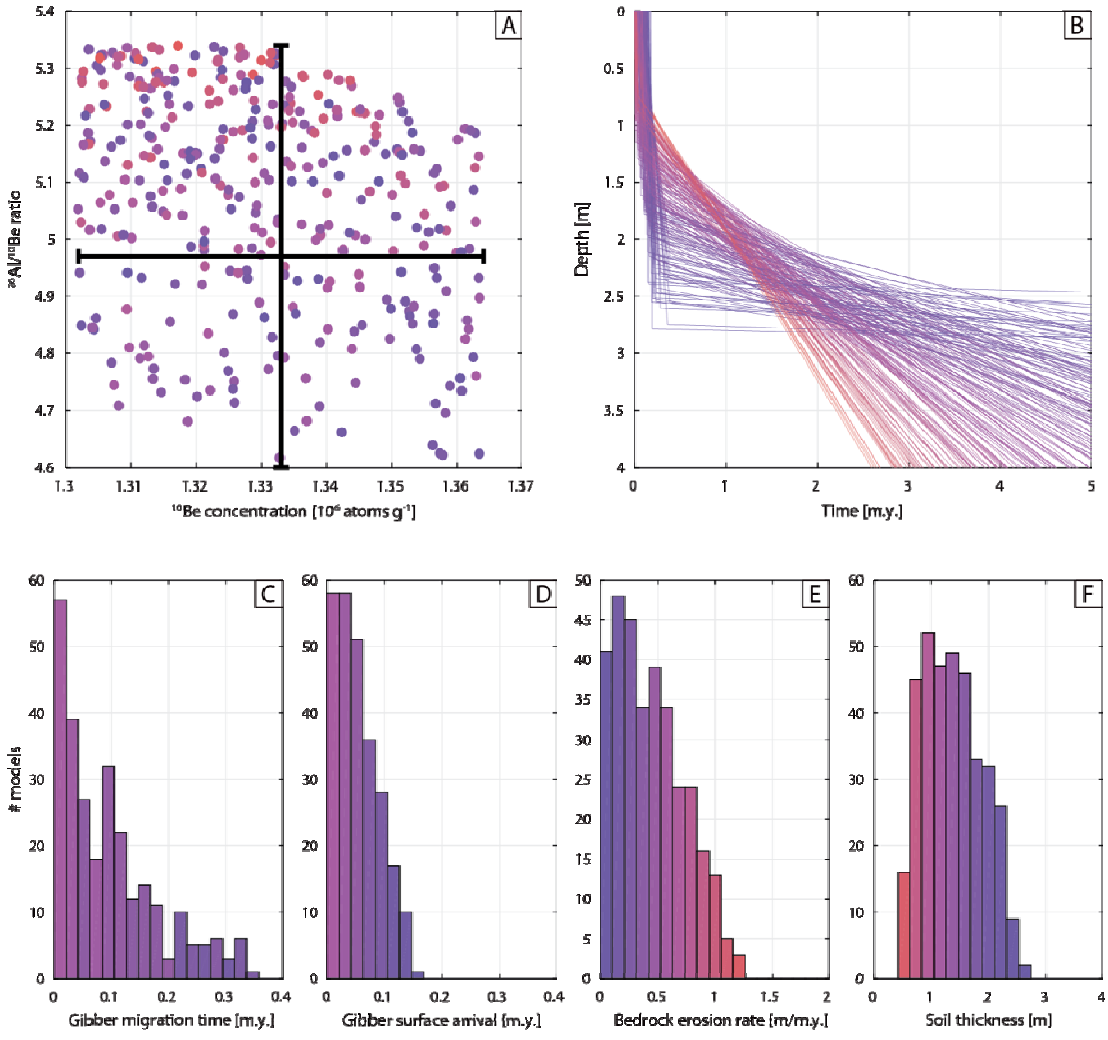

II

NIL-TS4

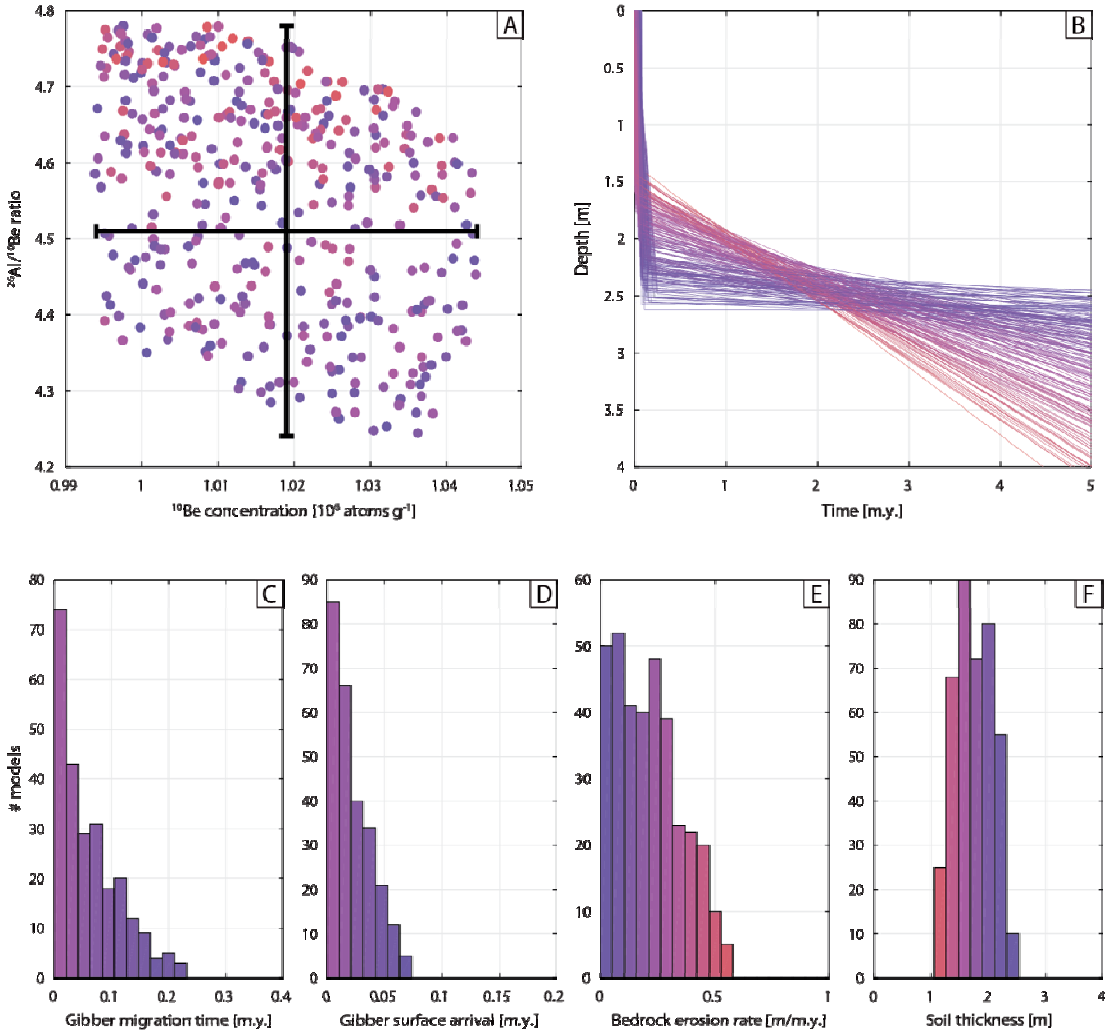
A
B
C
D
E
F
$^{26}Al/^{10}Be$ ratio
^{10}Be concentration [10^6 atoms g^{-1}]
Depth [m]
Time [m.y.]
models
Gibber migration time [m.y.]
Gibber surface arrival [m.y.]
Bedrock erosion rate [m/m.y.]
Soil thickness [m]

III

NIL-TS6

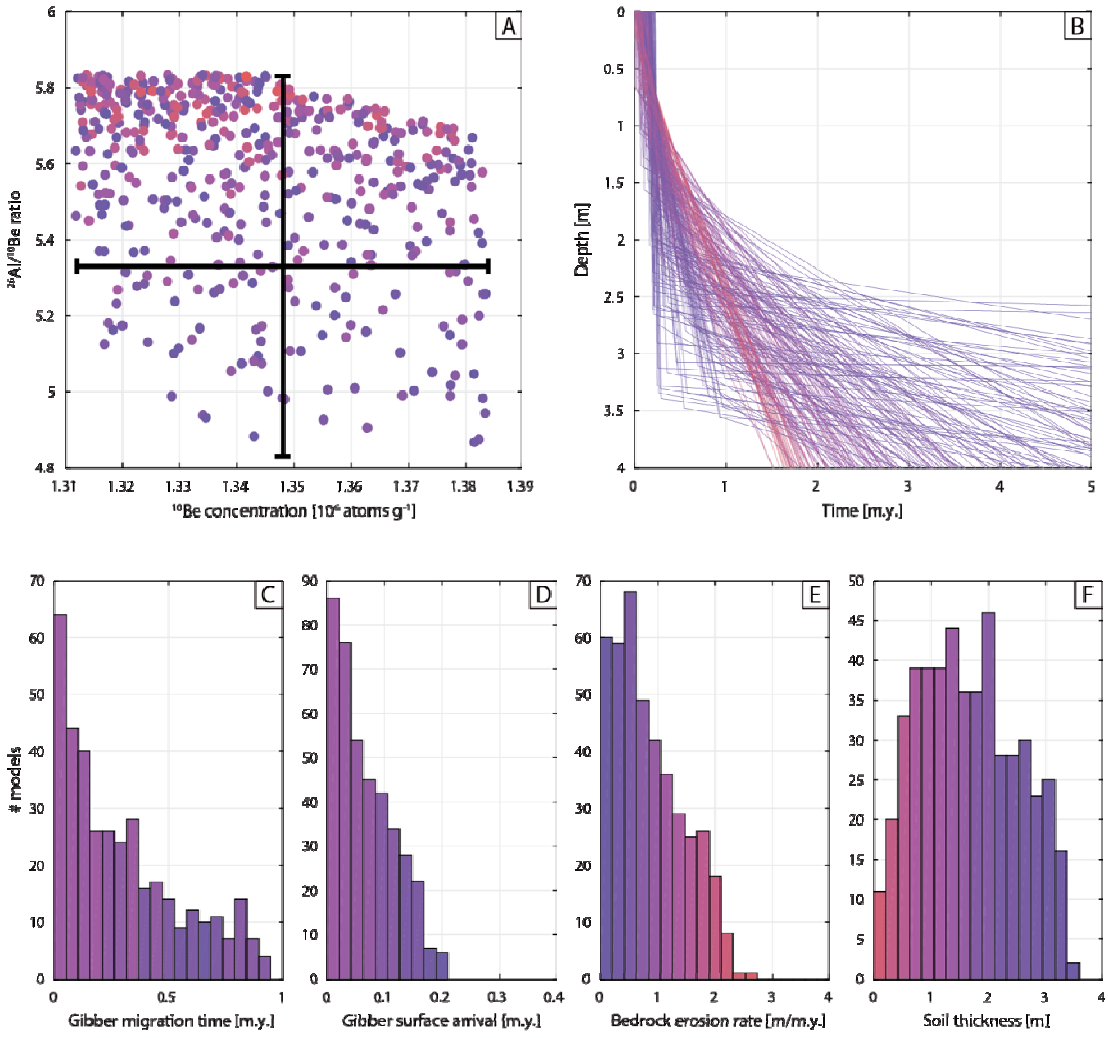
A
$^{26}Al/^{10}Be$ ratio
^{10}Be concentration [10^6 atoms g^{-1}]
B
Depth [m]
Time [m.y.]
C
models
Gibber migration time [m.y.]
D
Gibber surface arrival [m.y.]
E
Bedrock erosion rate [m/m.y.]
F
Soil thickness [m]

IV

NIL-TS8

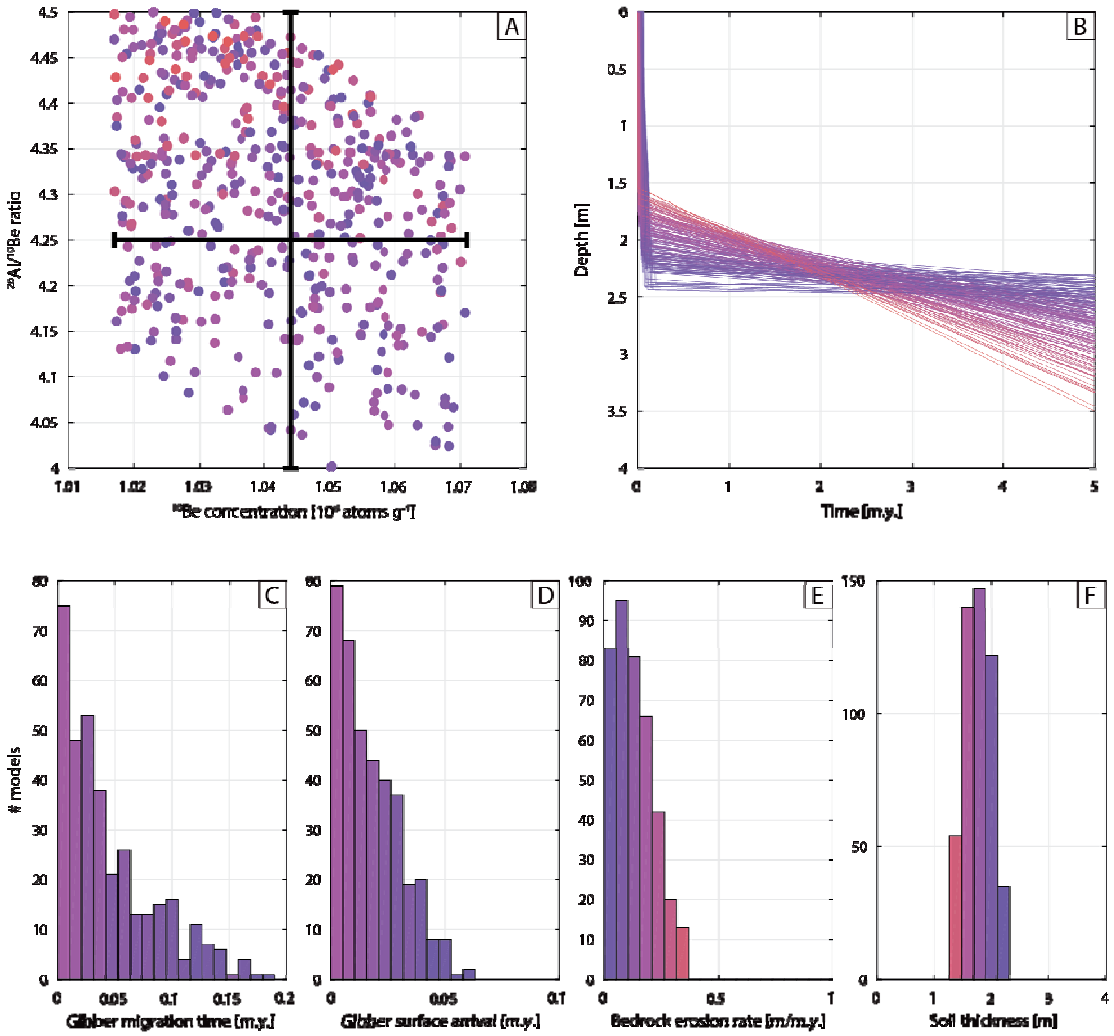
A
B
C
D
E
F
$^{26}Al/^{10}Be$ ratio
^{10}Be concentration [10^4 atoms g^{-1}]
Depth [m]
Time [m.y.]
models
Gibber migration time [m.y.]
Gibber surface arrival [m.y.]
Bedrock erosion rate [m/m.y.]
Soil thickness [m]

v

NIL-TS10

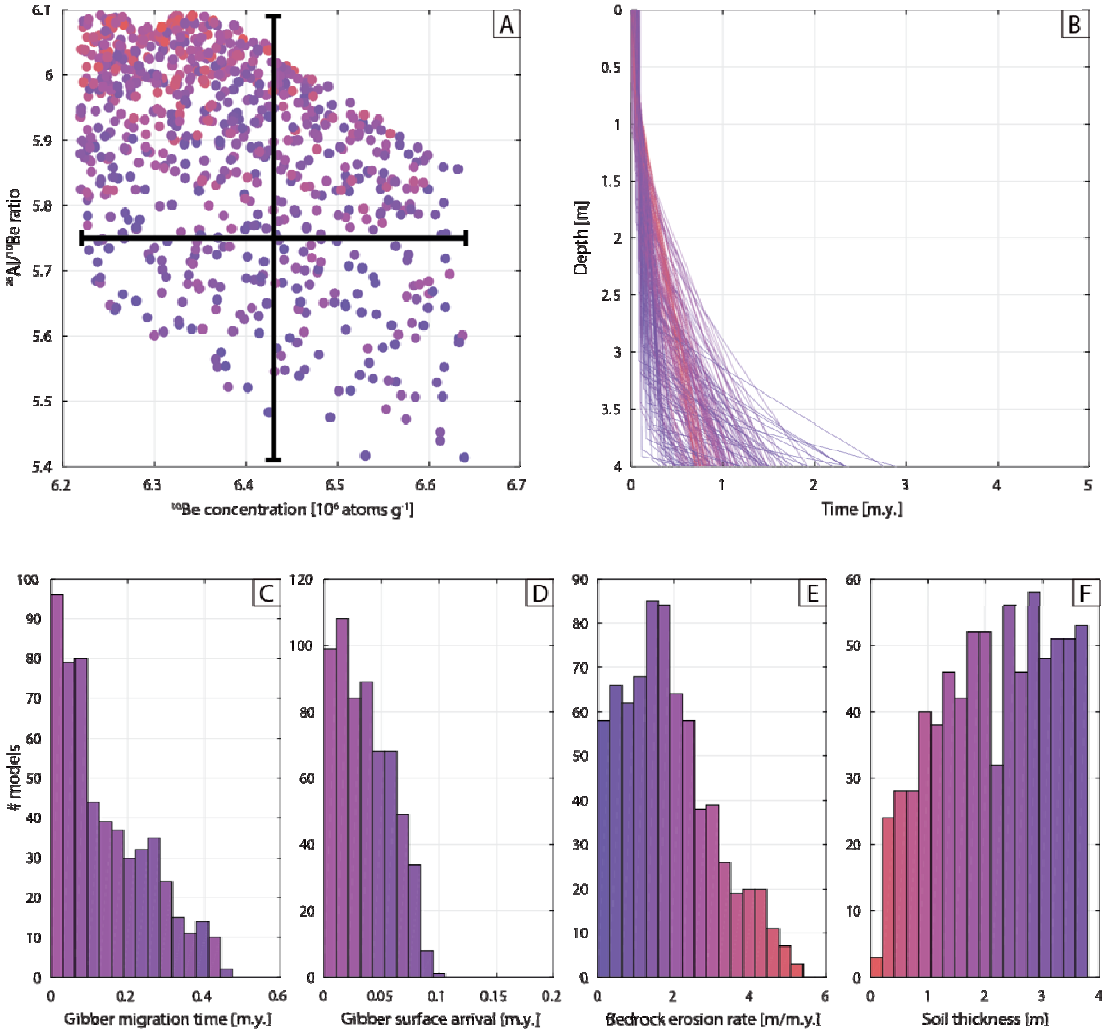
A
B
C
D
E
F
$^{26}Al/^{10}Be$ ratio
^{10}Be concentration [10^6 atoms g^{-1}]
Depth [m]
Time [m.y.]
models
Gibber migration time [m.y.]
Gibber surface arrival [m.y.]
Bedrock erosion rate [m/m.y.]
Soil thickness [m]

VI

TD-TS1

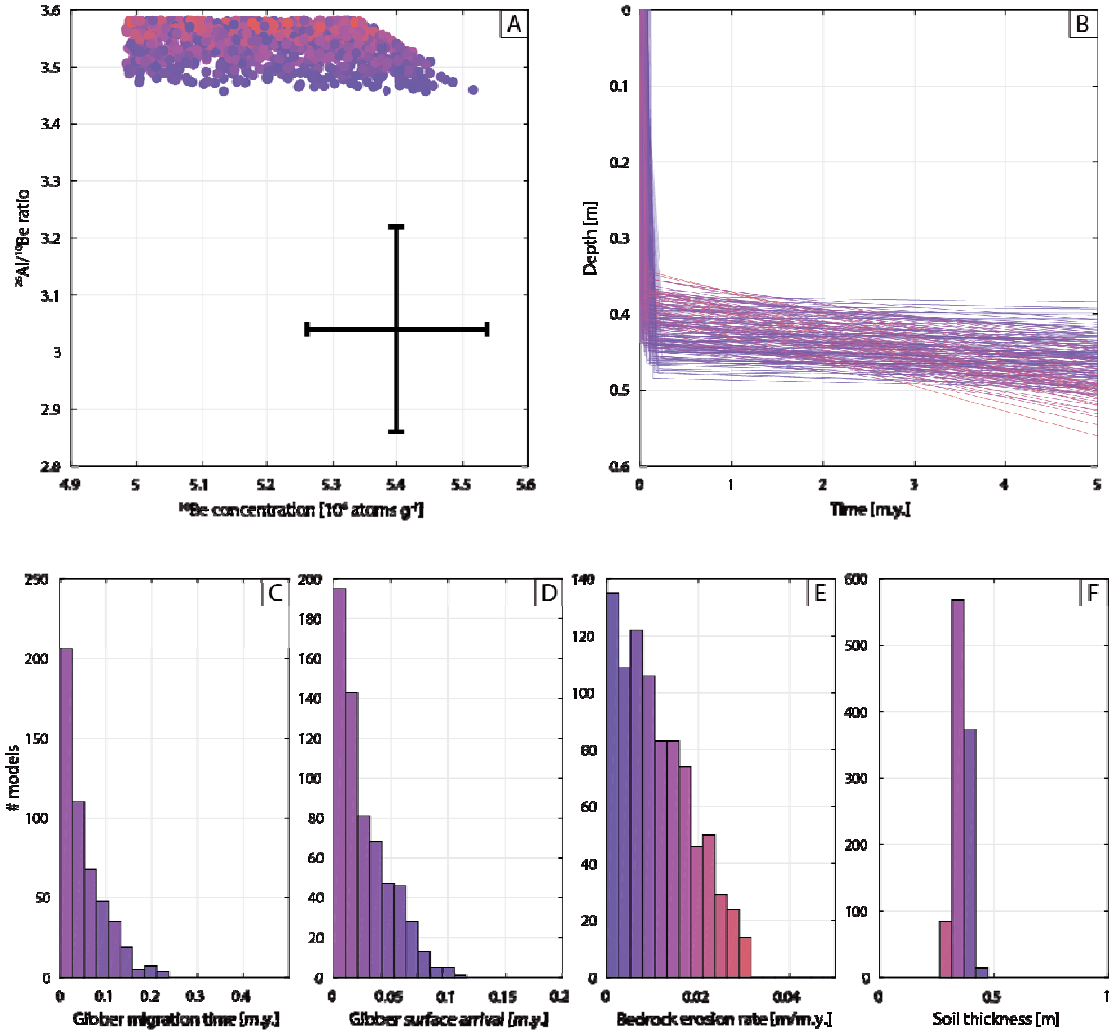
A
B
C
D
E
F
$^{26}Al/^{10}Be$ ratio
^{10}Be concentration [10^4 atoms g^{-1}]
Depth [m]
Time [m.y.]
models
Gibber migration time [m.y.]
Gibber surface arrival [m.y.]
Bedrock erosion rate [m/m.y.]
Soil thickness [m]

VII

TD-TS4

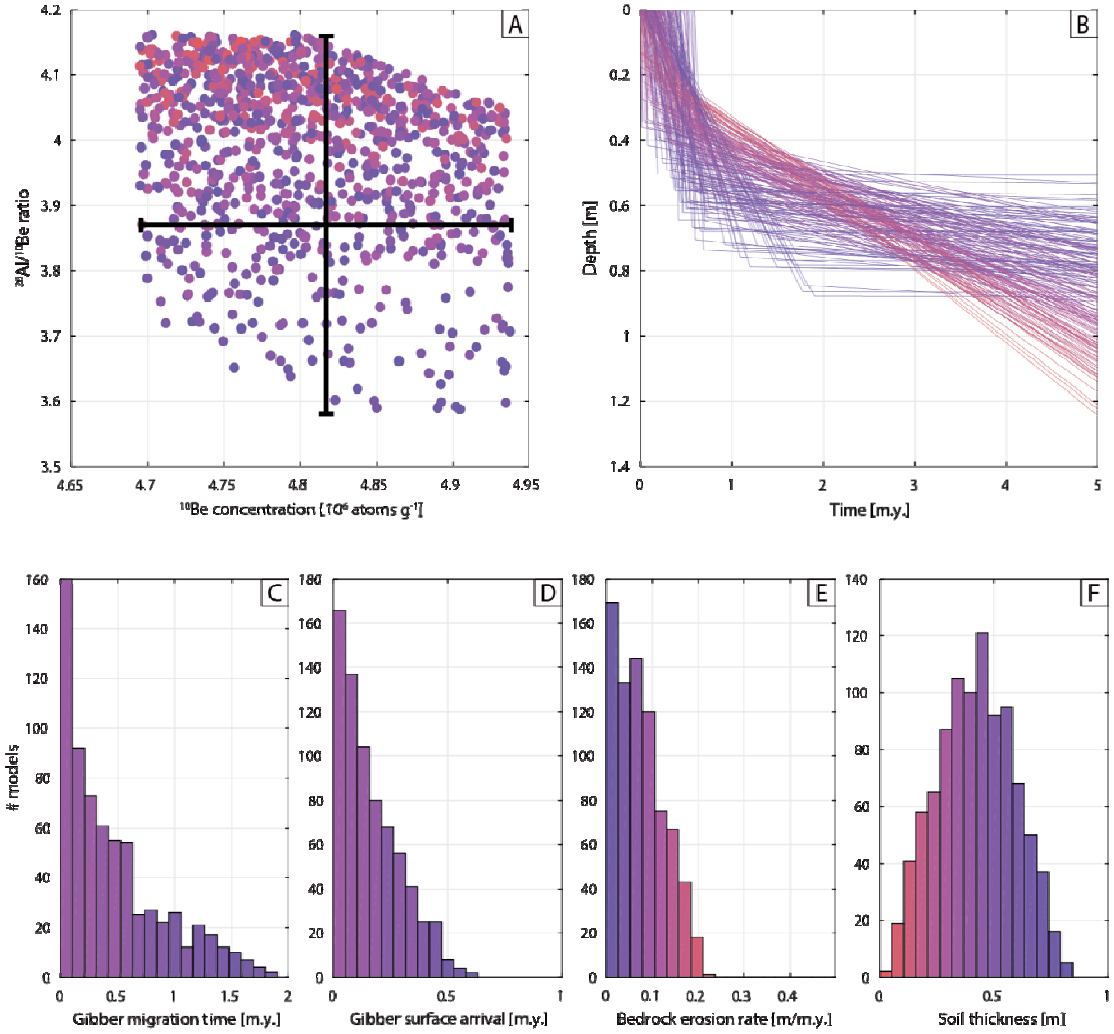
A
B
C
D
E
F
$^{26}Al/^{10}Be$ ratio
^{10}Be concentration [10^6 atoms g^{-1}]
Depth [m]
Time [m.y.]
models
Gibber migration time [m.y.]
Gibber surface arrival [m.y.]
Bedrock erosion rate [m/m.y.]
Soil thickness [m]

VIII

TD-TS9

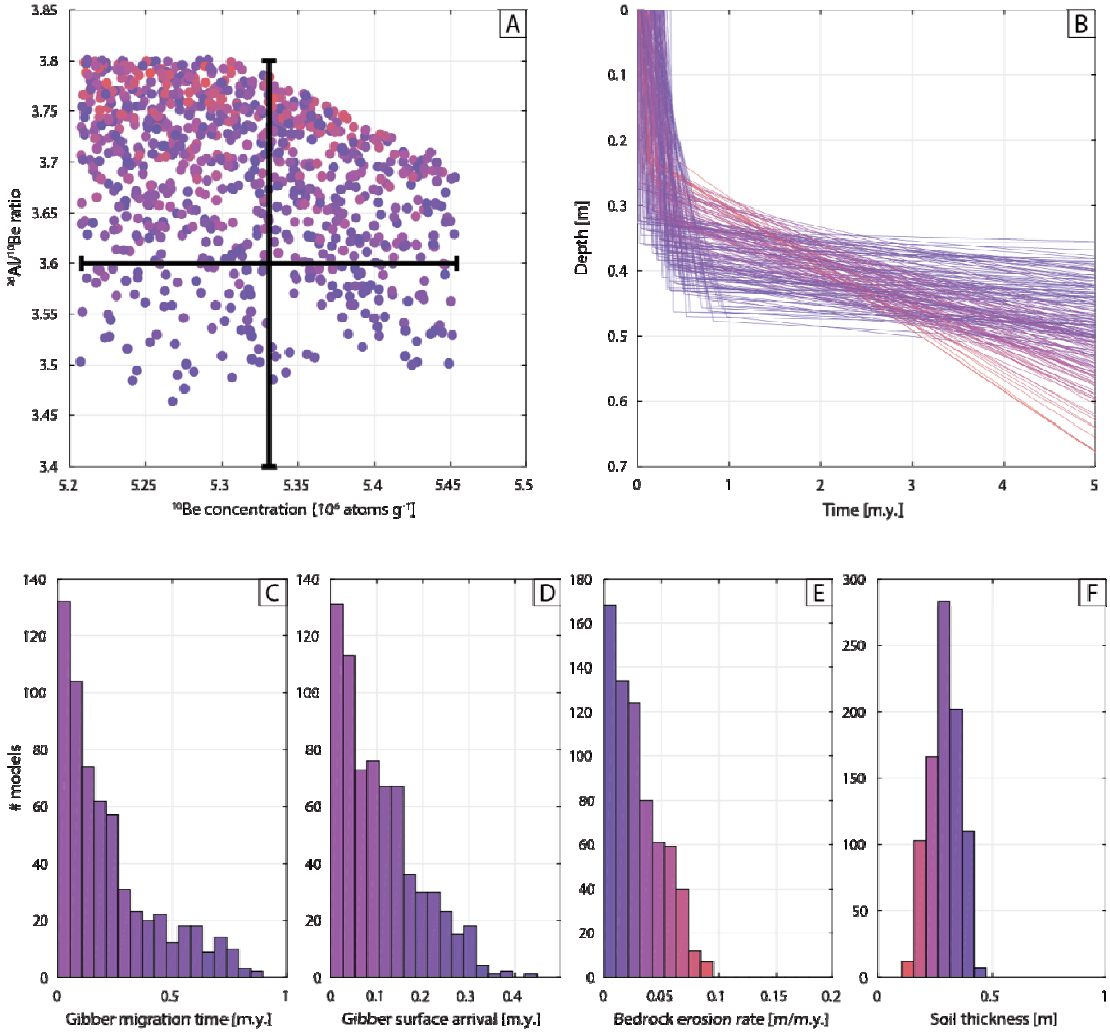
A
B
C
D
E
F
$^{26}Al/^{10}Be$ ratio
^{10}Be concentration [10^4 atoms g^{-1}]
Depth [m]
Time [m.y.]
models
Gibber migration time [m.y.]
Gibber surface arrival [m.y.]
Bedrock erosion rate [m/m.y.]
Soil thickness [m]

IX

PIO-TS5

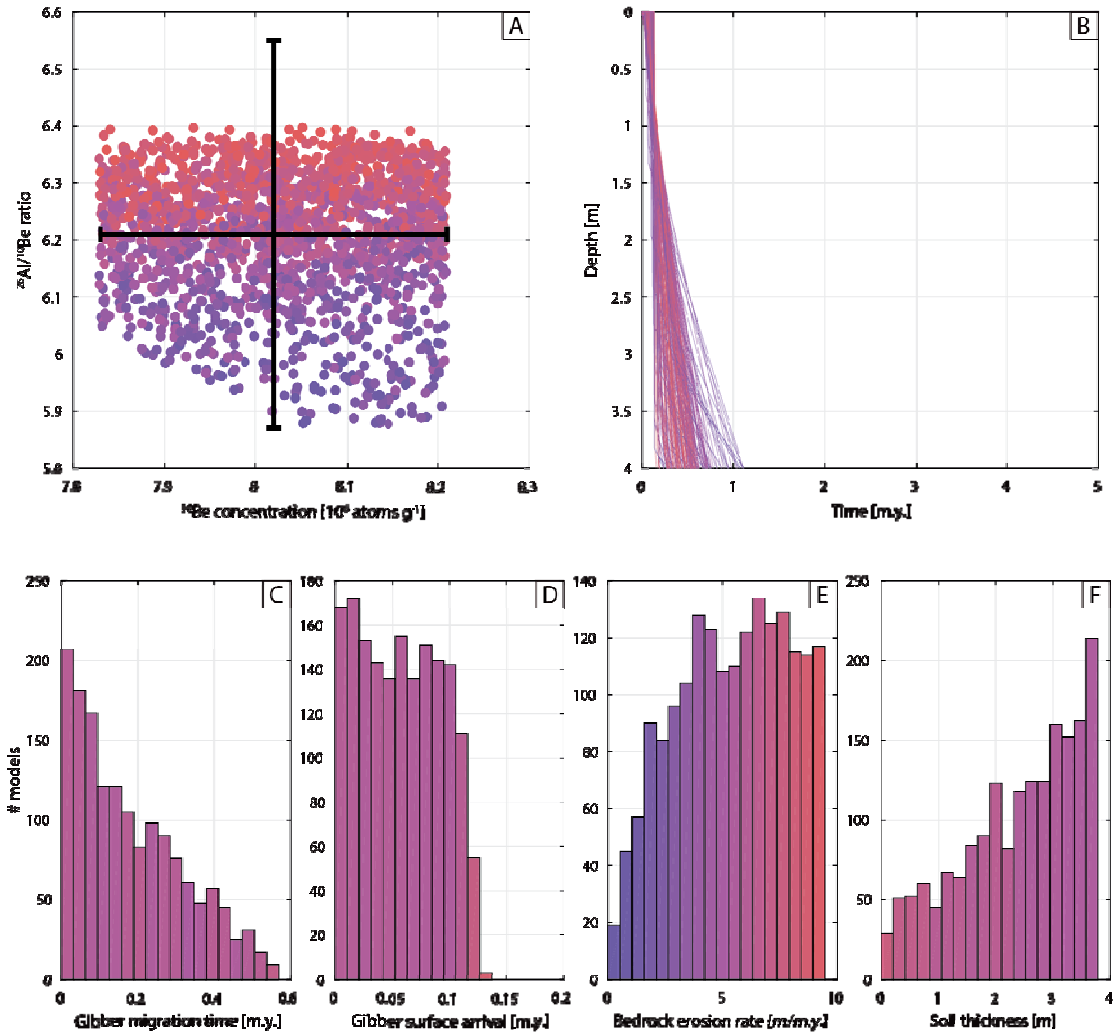
A
B
C
D
E
F
$^{26}Al/^{10}Be$ ratio
^{10}Be concentration [10^6 atoms g^{-1}]
Depth [m]
Time [m.y.]
models
Gibber migration time [m.y.]
Gibber surface arrival [m.y.]
Bedrock erosion rate [m/m.y.]
Soil thickness [m]

PIO-TS7

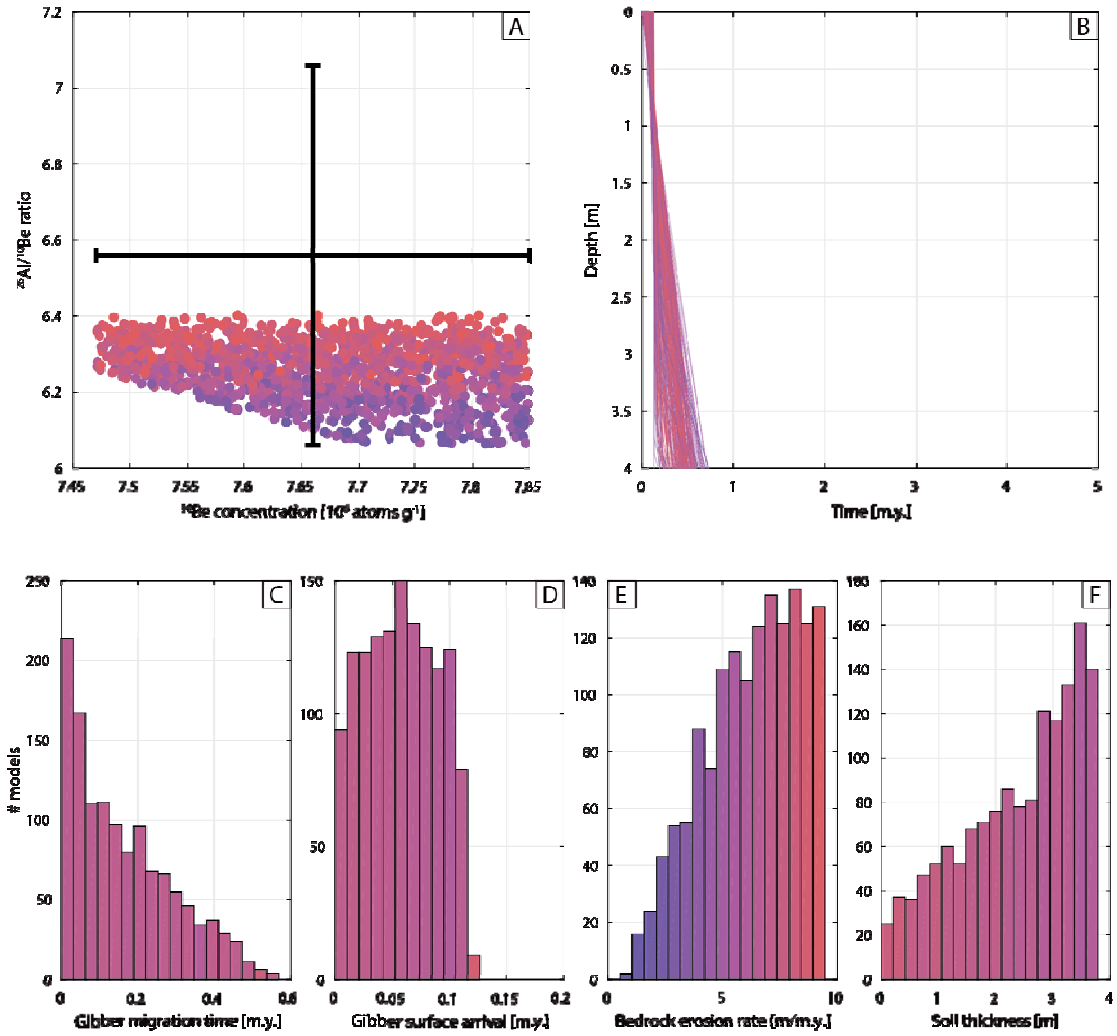
A
B
C
D
E
F
$^{26}Al/^{10}Be$ ratio
^{10}Be concentration [10^6 atoms g^{-1}]
Depth [m]
Time [m.y.]
models
Gibber migration time [m.y.]
Gibber surface arrival [m.y.]
Bedrock erosion rate [m/m.y.]
Soil thickness [m]

XI

PIO-TS9

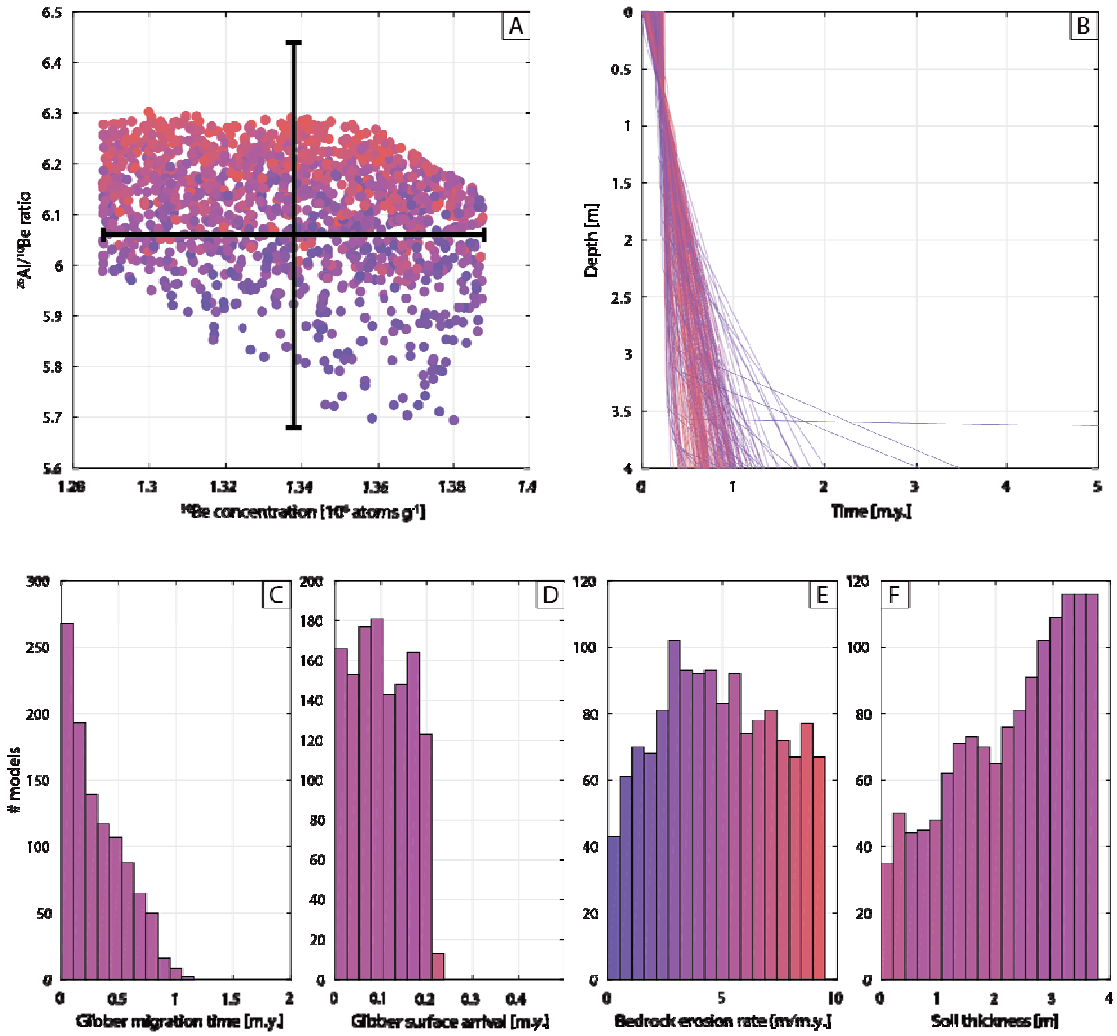
A
B
C
D
E
F
$^{26}Al/^{10}Be$ ratio
^{10}Be concentration [10^6 atoms g^{-1}]
Depth [m]
Time [m.y.]
models
Glibber migration time [m.y.]
Glibber surface arrival [m.y.]
Bedrock erosion rate [m/m.y.]
Soil thickness [m]

Figure DR8: The 'overcomplicated' MC6 (6-parameter) Monte Carlo-based inversion model outputs for paired NIL-TOP-0 and NIL-TOP-70 samples. A) and B) The $^{26}Al/^{10}Be$ (±1σ uncertainty) domain that defines the accepted forward models for NIL-TOP-0 (red) and NIL-TOP-70 (blue). C) Exhumation paths of accepted models spanning the past 4 Ma. Note the additional particle burial due to soil accretion ~1.5–0.5 m.y. The six free-parameters are: D) initial soil thickness, E) soil accretion thickness, F) soil accretion time (Tr), G) time of gibber bedrock detachment at base of soil (Tp), H) gibber arrival time at soil surface (Ta), and I) bedrock erosion rate at the base of soil (Erate).

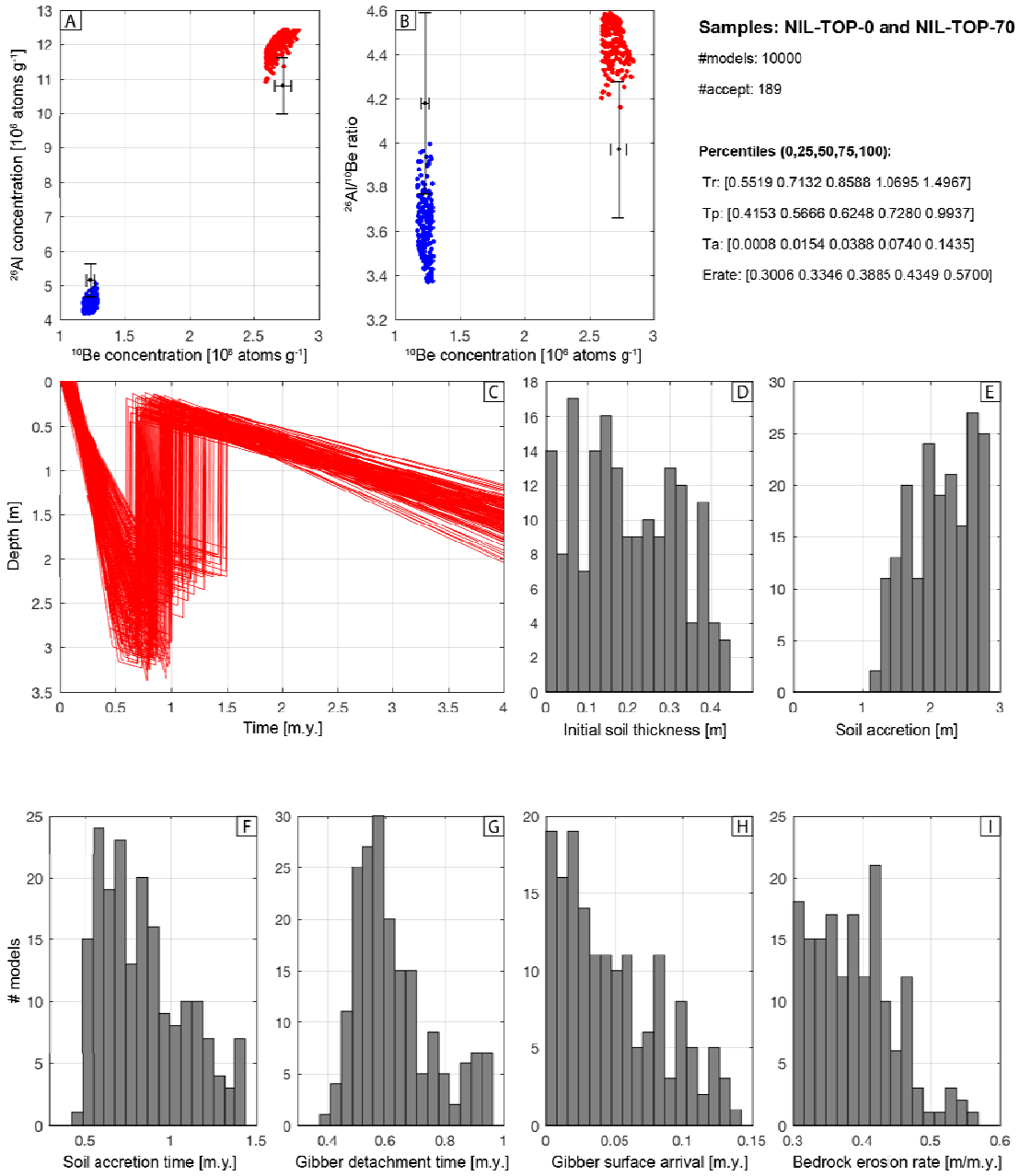

Table DR1: Summary of depth-profile related Monte Carlo model parameters.

Site and nuclide specific information	**^{10}Be**	**^{26}Al**
Latitude (decimal deg.)	-23.7112	-23.7112
Longitude (decimal deg.)	132.7867	132.7867
Altitude (m a.s.l.)	702.7	702.7
Shielding		
Topographic shielding	0.9996	0.9996
Cover	1	1
^{10}Be and ^{26}Al production rate		
Spallation production	5.21	34.9
Bulk material density		
Minimum density	1.5	1.5
Maximum density	1.9	1.9
Monte Carlo parameters[a)]		
chi-squared value	12[b)]	4[b)]
Number of profiles	100000	100000
Min age (y.)	140000	100000
Max age (y.)	330000	400000
Min erosion rate (cm/k.y.)	0	0
Max erosion rate (cm/k.y.)	1	1
Min total erosion threshold (cm)	0	0
Max total erosion threshold (cm)	50	50
Min inheritance (atoms/g)	350000	1500000
Max inheritance (atoms/g)	620000	3500000
Neutrons (mean value)	160	160
Neutrons (standard deviation)	5	5

a) For explanation of parameters see (Hidy et al., 2010).
b) No solutions were found for lower chi-squared values.

Table DR2: Grain size characteristics of fine-grained plateau sediment at Mt Margaret.

Sample ID	Depth [cm]	Mean grain size [µm]	Standard deviation [µm]	Sand content [%]	Silt content [%]	Clay content [%]	Medium/Coarse silt (20-50 µm) [%]
NIL-TOP-10	10	42.8	6.5	18.2	73.2	8.6	46.3
NIL-TOP-30	30	41.7	6.4	16.1	74.9	9.0	44.9
NIL-TOP-50	50	34.1	5.8	12.7	72.0	15.3	28.6
NIL-TOP-70	70	30.2	5.4	13.4	64.3	22.3	13.5
Combined	***x***	***37.2***	***6.0***	***15.1***	***71.1***	***13.8***	***33.3***

Table DR3: Grain characteristics of colluvium pebbles.

Sample ID	Elevation [m a.s.l.]	Transect distance [m]	Slope surface images						CN sample images			
			A-axis[a] [cm]	B-axis[a] [cm]	Aspect ratio[a]	Circularity[a]	Perimeter[a] [cm]	Area[a] [cm^2]	A-axis[a] [cm]	B-axis[a] [cm]	Aspect ratio[a]	Circularity[a]
Mt Margaret[b]												
NIL-TS0	407.2	0	6.20 ± 4.37	3.73 ± 2.74	1.74 ± 0.55	0.74 ± 0.09	17.7 ± 12.7	26.5 ± 38.1	1.81 ± 0.32	1.25 ± 0.23	1.48 ± 0.34	0.74 ± 0.06
NIL-TS4	405.4	140.5	5.99 ± 4.07	3.55 ± 2.42	1.73 ± 0.51	0.73 ± 0.11	17.1 ± 11.4	23.2 ± 31.5	1.87 ± 0.32	1.31 ± 0.22	1.46 ± 0.31	0.70 ± 0.06
NIL-TS6	402.9	195.3	10.11 ± 5.89	5.96 ± 3.24	1.78 ± 0.63	0.72 ± 0.09	28.8 ± 15.8	58.6 ± 60.0	1.88 ± 0.38	1.30 ± 0.24	1.47 ± 0.32	0.70 ± 0.07
NIL-TS8	397.2	240.2	6.12 ± 5.08	3.39 ± 2.32	1.81 ± 0.52	0.73 ± 0.09	16.9 ± 13.4	24.5 ± 43.2	2.10 ± 0.40	1.36 ± 0.22	1.57 ± 0.40	0.70 ± 0.07
NIL-TS10	387.2	286.4	6.32 ± 5.22	3.45 ± 2.47	1.77 ± 0.54	0.73 ± 0.09	17.5 ± 13.6	26.0 ± 35.8	2.11 ± 0.42	1.48 ± 0.22	1.44 ± 0.31	0.69 ± 0.08
Combined	***x***	***x***	***6.90 ± 5.17***	***3.99 ± 2.81***	***1.77 ± 0.55***	***0.73 ± 0.09***	***19.5 ± 14.1***	***31.4 ± 44.3***	***1.95 ± 0.39***	***1.33 ± 0.24***	***1.48 ± 0.34***	***0.71 ± 0.07***
NIL-TOP-0	406	x	x	x	x	x	x	x	7.99 ± 1.60	5.65 ± 0.75	1.42 ± 0.26	0.64 ± 0.09
Coongra[b]												
TD-TS0	275	0	5.08 ± 6.68	3.65 ± 4.35	1.39 ± 0.27	0.81 ± 0.07	15.2 ± 20.0	36.3 ± 127.9	x	x	x	x
TD-TS1	**270**	**220.8**	**5.39 ± 4.57**	**3.85 ± 3.41**	**1.46 ± 0.33**	**0.80 ± 0.08**	**16.1 ± 14.1**	**28.0 ± 56.2**	**1.75 ± 0.24**	**1.35 ± 0.20**	**1.31 ± 0.19**	**0.81 ± 0.04**
TD-TS2	262.6	441.6	7.06 ± 6.49	5.07 ± 4.75	1.41 ± 0.27	0.80 ± 0.07	21.1 ± 19.6	51.3 ± 111.9	x	x	x	x
TD-TS3	246.5	714.6	7.32 ± 5.97	5.19 ± 3.94	1.45 ± 0.41	0.82 ± 0.07	21.4 ± 17.0	46.9 ± 81.3	x	x	x	x
TD-TS4	**236.8**	**938.7**	**5.17 ± 3.08**	**3.47 ± 2.07**	**1.52 ± 0.41**	**0.80 ± 0.07**	**14.8 ± 8.6**	**18.6 ± 20.9**	**1.74 ± 0.27**	**1.33 ± 0.20**	**1.31 ± 0.20**	**0.80 ± 0.04**
TD-TS5	228.4	1206.7	6.27 ± 6.29	4.46 ± 4.89	1.47 ± 0.31	0.80 ± 0.06	18.6 ± 19.7	45.5 ± 145.0	x	x	x	x
TD-TS6	221.8	1443	5.35 ± 5.47	3.81 ± 3.88	1.40 ± 0.33	0.81 ± 0.07	15.9 ± 16.5	32.0 ± 88.9	x	x	x	x
TD-TS7	213.4	1724.5	4.41 ± 3.01	3.10 ± 2.08	1.46 ± 0.30	0.81 ± 0.06	13.0 ± 8.8	15.3 ± 21.9	x	x	x	x
TD-TS8	208.3	1943.6	5.80 ± 4.61	4.19 ± 3.58	1.46 ± 0.40	0.79 ± 0.08	17.5 ± 14.5	31.3 ± 59.3	x	x	x	x
TD-TS9	**201.3**	**2201.2**	**5.52 ± 2.98**	**3.92 ± 2.17**	**1.45 ± 0.30**	**0.80 ± 0.07**	**16.3 ± 8.8**	**21.7 ± 21.7**	**1.79 ± 0.31**	**1.39 ± 0.21**	**1.29 ± 0.18**	**0.82 ± 0.04**
Combined			***5.76 ± 5.31***	***4.09 ± 3.79***	***1.44 ± 0.33***	***0.80 ± 0.07***	***17.1 ± 16.0***	***33.6 ± 89.7***	***1.76 ± 0.27***	***1.36 ± 0.20***	***1.32 ± 0.20***	***0.81 ± 0.05***
Pioneer[b]												
PIO-TS5	707.4	40.4	4.72 ± 4.43	3.07 ± 3.07	1.59 ± 0.42	0.77 ± 0.08	13.7 ± 13.0	21.3 ± 48.9	6.46 ± 0.86	4.67 ± 0.58	1.39 ± 0.18	0.74 ± 0.04
PIO-TS7	705.2	60.6	4.27 ± 2.87	2.95 ± 1.98	1.50 ± 0.36	0.79 ± 0.07	12.5 ± 8.2	13.9 ± 21.7	6.74 ± 0.70	4.86 ± 0.51	1.39 ± 0.14	0.75 ± 0.06
PIO-TS9	703.9	86.7	3.49 ± 2.80	2.42 ± 1.93	1.47 ± 0.31	0.80 ± 0.07	10.3 ± 8.2	10.66 ± 20.2	6.69 ± 0.73	4.78 ± 0.57	1.41 ± 0.19	0.75 ± 0.05
PIO-TS11	702.7	126.1	x	x	x	x	x	x	5.76 ± 1.05	4.63 ± 1.00	1.26 ± 0.21	0.78 ± 0.04
PIO-TS13	701.9	152.9	3.43 ± 2.49	2.41 ± 1.72	1.44 ± 0.30	0.80 ± 0.06	10.1 ± 7.1	9.7 ± 16.2	6.71 ± 0.73	5.06 ± 0.87	1.36 ± 0.27	0.76 ± 0.06
PIO-TS17	700.1	214	2.00 ± 1.37	1.43 ± 1.05	1.43 ± 0.26	0.81 ± 0.06	5.9 ± 4.2	3.3 ± 6.0	6.59 ± 0.87	4.91 ± 0.71	1.36 ± 0.20	0.77 ± 0.04
PIO-TS18	699.1	250.5	2.29 ± 1.85	1.64 ± 1.33	1.41 ± 0.28	0.82 ± 0.06	6.8 ± 5.4	4.8 ± 8.3	6.66 ± 1.08	4.93 ± 0.80	1.37 ± 0.21	0.76 ± 0.04
Combined			***3.36 ± 2.95***	***2.31 ± 2.03***	***1.47 ± 0.33***	***0.80 ± 0.07***	***9.8 ± 8.6***	***10.6 ± 25.2***	***6.53 ± 0.90***	***4.83 ± 0.72***	***1.37 ± 0.20***	***0.76 ± 0.05***
PIO-TS11 / DP0	702.7	126.1	x	x	x	x	x	x	5.76 ± 1.05	4.63 ± 1.00	1.26 ± 0.21	0.78 ± 0.04
PIO-DP30	702.4	126.1	x	x	x	x	x	x	6.13 ± 1.44	4.69 ± 1.13	1.33 ± 0.28	0.75 ± 0.05
PIO-DP60	702.1	126.1	x	x	x	x	x	x	7.41 ± 1.82	4.57 ± 0.94	1.66 ± 0.48	0.68 ± 0.07
PIO-DP100	701.7	126.1	x	x	x	x	x	x	6.58 ± 1.52	4.20 ± 0.72	1.57 ± 0.26	0.73 ± 0.05
PIO-DP150	701.2	126.1	x	x	x	x	x	x	6.58 ± 1.27	4.64 ± 0.80	1.46 ± 0.39	0.73 ± 0.06
PIO-DP200	700.7	126.1	x	x	x	x	x	x	6.74 ± 1.67	5.08 ± 0.82	1.33 ± 0.22	0.75 ± 0.05
PIO-DP250	700.2	126.1	x	x	x	x	x	x	7.50 ± 1.89	4.96 ± 1.58	1.60 ± 0.49	0.71 ± 0.06
PIO-DP285	699.85	126.1	x	x	x	x	x	x	8.11 ± 1.71	5.79 ± 1.44	1.43 ± 0.24	0.74 ± 0.05
Combined			***x***	***x***	***x***	***x***	***x***	***x***	***6.77 ± 1.65***	***4.77 ± 1.10***	***1.45 ± 0.35***	***0.73 ± 0.06***

a) Uncertainties expressed at 1-sigma level

b) Minimum B-axes measured in slope surface pictures are 0.46 cm (Mt Margaret), 0.44 cm (Coongra), and 0.30 cm (Pioneer)

References Cited

Hidy, A. J., Gosse, J. C., Pederson, J. L., Mattern, J. P., and Finkel, R. C., 2010, A geologically constrained Monte Carlo approach to modeling exposure ages from profiles of cosmogenic nuclides: An example from Lees Ferry, Arizona: Geochemistry, Geophysics, Geosystems, v. 11, doi:10.1029/2010gc003084.